Received: 1 September 2022 | Revised: 6 February 2023 | Accepted: 8 February 2023

DOI: 10.1002/bip.23532

ARTICLE

Biopolymers WILEY

Sorghum bicolor *Sb*HSP110 has an elongated shape and is able of protecting against aggregation and replacing human HSPH1/HSP110 in refolding and disaggregation assays

Juliana C. Franco[1] | Maria L. C. Nogueira[1] | Gabriela M. Gandelini[1] | Glaucia M. S. Pinheiro[1] | Conrado C. Gonçalves[1] | Leandro R. S. Barbosa[2,3] | Jason C. Young[4†] | Carlos H. I. Ramos[1,5]

[1]Institute of Chemistry, University of Campinas UNICAMP, Campinas, SP, Brazil

[2]Institute of Physics, University of São Paulo, São Paulo, SP, Brazil

[3]Brazilian Synchrotron Light Laboratory (LNLS), Brazilian Center for Research in Energy and Materials (CNPEM), Campinas, SP, Brazil

[4]Department of Biochemistry, McGill University, Montreal, Quebec, Canada

[5]National Institute of Science & Technology of Structural Biology and Bioimage (INCTBEB), Rio de Janeiro, Brazil

Correspondence
Carlos H. I. Ramos, Institute of Chemistry, University of Campinas UNICAMP, Campinas, SP 13083-970, Brazil.
Email: cramos@unicamp.br

Funding information
Conselho Nacional de Desenvolvimento Científico e Tecnológico, Grant/Award Numbers: 305148-2019-2, 309418/2021-6; FAPESP, Grant/Award Numbers: 2012/50161-8, 2016/02137-1, 2016/03764-0, 2016/14503-2, 2017/26131-5, 2018/11948-9, 2016/04246-2

Abstract

Perturbations in the native structure, often caused by stressing cellular conditions, not only impair protein function but also lead to the formation of aggregates, which can accumulate in the cell leading to harmful effects. Some organisms, such as plants, express the molecular chaperone HSP100 (homologous to HSP104 from yeast), which has the remarkable capacity to disaggregate and reactivate proteins. Recently, studies with animal cells, which lack a canonical HSP100, have identified the involvement of a distinct system composed of HSP70/HSP40 that needs the assistance of HSP110 to efficiently perform protein breakdown. As sessile plants experience stressful conditions more severe than those experienced by animals, we asked whether a plant HSP110 could also play a role in collaborating with HSP70/HSP40 in a system that increases the efficiency of disaggregation. Thus, the gene for a putative HSP110 from the cereal *Sorghum bicolor* was cloned and the protein, named SbHSP110, purified. For comparison purposes, human HsHSP110 (HSPH1/HSP105) was also purified and investigated in parallel. First, a combination of spectroscopic and hydrodynamic techniques was used for the characterization of the conformation and stability of recombinant SbHSP110, which was produced folded. Second, small-angle X-ray scattering and combined predictors of protein structure indicated that SbHSP110 and HsHSP110 have similar conformations. Then, the chaperone activities, which included protection against aggregation, refolding, and reactivation, were investigated, showing that SbHSP110 and HsHSP110 have similar functional activities. Altogether, the results add to the structure/function relationship study of HSP110s and support the hypothesis that plants have multiple strategies to act upon the reactivation of protein aggregates.

KEYWORDS
HSP70 heat shock protein, molecular chaperones, protein aggregates, protein disaggregation, HSP110

Abbreviations: Bis-ANS, 4,4′-dianilino-1,1′-binaphthyl-5,5′-disulfonic acid; CD, circular dichroism; CS, citrate synthase; HSP, heat shock protein; Ins, insulin; Luc, luciferase; MD, malate dehydrogenase; NBD, nucleotide-binding domain; NEF, nucleotide exchange factor; SAXS, small-angle X-ray scattering; SBD, substrate-binding domain; SEC-MALS, size exclusion chromatography coupled to multi-angle light scattering.

Juliana C. Franco and Maria L. C. Nogueira contributed equally to this work.

† In memoriam.

1 | INTRODUCTION

Protein misfolding followed by aggregation is a process that may be spontaneous or caused by stressful conditions but nonetheless contributes to cellular aging and many diseases.[1–3] To avoid these harmful situations, cells developed mechanisms, such as those constituted by molecular chaperones and Heat Shock Proteins (HSPs), to rescue defective proteins by helping them to reactivate and reach their correct fold.[4–7] Unsurprisingly, several HSP families are ubiquitous and are involved in helping nascent protein folding and translocation and thus avoiding misfolding and aggregation. Considering the main functions, HSP families can be classified into foldases, which aid folding, such as HSP70 and HSP90; holders, that protect protein against aggregation, such as SmHSP (small HSP); and disaggregases, which are involved in reactivating aggregates, such as HSP100.[7,8] Foldases and disagregases are ATPases, and thus have ATP-dependent activity, whereas holders have ATP-independent activity. Additionally, certain HSPs are multifunctional, such as HSP70, which has foldase, disaggregase, and holder-like activities.

HSP70, 70 kDa HSP, is one of the most important chaperones because it participates in the protection of proteostasis by aiding folding and avoiding misfolding (for reviews see Reference [9–12]) HSP70s are aided by many co-chaperones, mainly those from the HSP40/DNAJ family, which is characterized by a conserved J-domain, has holder activity, and is involved in delivering substrate and in ATPase stimulation.[13,14] Other co-chaperones, also known as nucleotide exchange factors (NEFs), are also important in these situations by helping HSP70 to recover its ATP-binding state.[15–17] In eukaryotes, such function is performed by BAG and HSP110.[18,19] Human HSP110, also named HSPH1 and HSP105, is a cytosolic chaperone that can act as a nucleotide exchange factor for HSP70s by binding to the nucleotide binding domain (NBD) of HSP70/HSPA1A.[17] In agreement, the yeast HSP110 homologous Sse1/2 also interacts with Ssa (HSP70) via its NDB and promotes nucleotide exchange.[20] A plant HSP110, AtHSP70-15, was first identified almost three decades ago in *Arabidopsis thaliana*.[21] The combination of HSP110s and HSP70s constitute a HSP70 superfamily as much of their structure and function characteristics can be deduced from sequence comparison.[22]

HSP110s are also involved in other relevant functions. For instance, it cooperates with HSP70 and HSP40 to form a HSP70-based machinery that stimulates protein disaggregation and reactivation.[23–30] Disaggregase machineries are ATP-dependent and have potent disaggregation and reactivation activities. In such machinery, human HSP110s (HSP105 and HSPA4/Apg-2) are essential to promote disaggregation, a result also shown for yeast Sse1/HSP70, even though this organism express a canonical HSP100 disaggregase, HSP104.[23] Recently, it was shown that a human SmHSP, HSPB-1, increase significantly the efficacy of the HSP70/HSP110/HSP40 machinery in recovering protein aggregates (Figure 1[31]).

The results with HSP70-based machinery are impressive because until recently only chaperones from the HSP100 family (for instance, CLPB in *Escherichia coli* and HSP104 in yeast) were known to act as disaggregases, and no representatives of this protein was found in metazoan.[8,23,32] Plants are among the organisms that present the canonical disaggregase HSP100[33,34] and it is scientifically important to explore their HSP70-based machinery. Therefore, we asked whether a HSP110 from sorghum has the same functions as that of a mammalian HSP110, both alone and as part of a previously identified HSP70-based machinery.[31] This work aims to investigate the hypothesis that plants, as yeast, improve proteostasis by having multiple disaggregase systems.

The mRNA sequence of human HSP105 was used to search the sequenced genome of *Sorghum bicolor*, one of the most important economical cereals in the world, to find its homologous in this organism. The gene, named here SbHSP110, was cloned and the recombinant protein was purified. Its conformation and function were determined, and the results were compared to those of a human HSP110, HsHSP110. Altogether, the findings herein are important because plants, by being sessile, experience stressful conditions that are more severe than those encountered, in general, by animals. By expressing a HSP110 that collaborates with the HSP70 system to increase the efficiency of their disaggregation machines, plants have another mechanism to cope with stress.

2 | MATERIALS AND METHODS

2.1 | Protein expression and purification

Human proteins studied in this work are HSP70 (HSC70, UNIPROT P11142), HSP110 (HSPH1/HSP105, UNIPROT Q92598), HSP40 (DNAJB4, UNIPROT Q9UDY4), and HSPB1-3D (HSPB1/SmHSP27, UNIPROT P04792, S15D/S78D/S82D triple mutant). In this work, they are referred as HSP70, HsHSP110, HSP40, and HSPB1-3D, respectively. The reference for HSP110 *S. bicolor*, named here SbHSP110, is XP_002439385.1 (NCBI). Recombinant human proteins HSP70, HSP40, and HSPB1-3D were purified as previously described.[35,36] SbHSP110 and HsHSP110 were expressed in *E. coli* BL21(DE3) in LB media and induced at $Abs_{600} \sim 0.7$ at 18°C for 4 h with IPTG 0.4–1 mM. Cells were harvested by centrifugation for 15 min at 2496 *g* and 4°C. Pellets were suspended in lysis buffer (Tris–HCl 50 mM pH 8.0, KCl 100 mM, EDTA 1 mM, DNase 5 units, PMSF 1 mM, and Lysozyme 30 μg mL^{-1}) and after 30 min of ice incubation, lysed by sonication (30 W, 5 s, 3×, 1 min between each step). His-tagged proteins were purified by Ni^{2+}-affinity chromatography (His-trap column, Cytiva). The fractions eluted with imidazole were submitted to Size Exclusion Chromatography (SEC). Final buffer for proteins was Tris–HCl 20 mmol L^{-1}; pH 7.5; NaCl 100 mmol L^{-1}; and beta-mercaptoethanol 1 mmol L^{-1}. Since the buffers used in the purification did not contain ATP and any ATP from the bacterial cell was likely removed during the process, ATP was added in specific experiments (such as SAXS, refolding and reactivation; see below). Unless stated otherwise the experiments were performed using buffer Tris–HCl 20 mmol L^{-1}; pH 7.5; NaCl 100 mmol L^{-1}; and beta-mercaptoethanol 1 mmol L^{-1}. Protein concentration was measured by the Edelhoch method[37] and purity was analyzed by SDS-PAGE. The client-proteins Citrate Synthase,

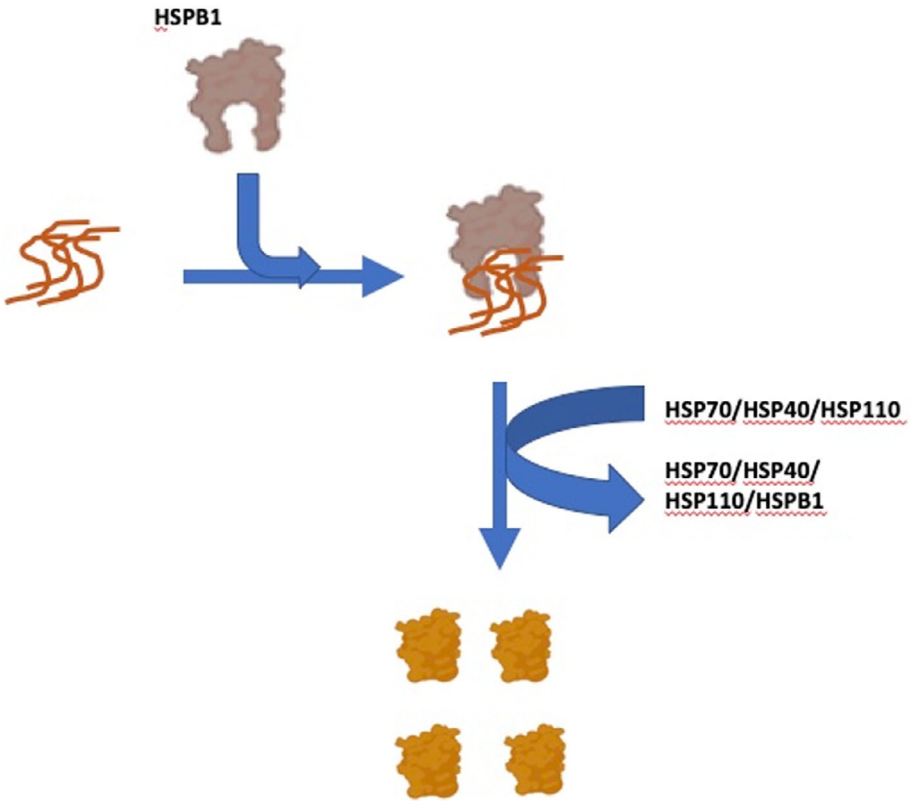

FIGURE 1 (a) HSP70/HSP40/HSP110/HSPB1 chaperone machinery for protein reactivation. Aggregated proteins associate with HSPB1 and are reactivated by the HSP70/HSP40/HSP110 chaperone machinery.[31] HSPB1 is essential for the resolubilization/reactivation of protein aggregates. The figure shows the fate of aggregated proteins under the action of the HSP70/HSP40/HSP110/HSPB1 machinery.

Luciferase, Insulin, Lysozyme, and Malate Dehydrogenase were from Sigma-Aldrich. All data shown in this work refer to the mean, with standard deviation, of at least three independent experiments.

2.2 | Analyses from the sequence

Analyses used online software. Alignment analyses were performed using NCBI, MUSCLE,[38] and ESpript[39] webservers; domain prediction was performed by SMART;[40] structure prediction analyses were performed using I-TASSER,[41] and PSIPRED;[42] and buffer viscosity was obtained using the Sednterp software.[43]

2.3 | Hydrodynamic studies

Size exclusion (SEC) and analytical size exclusion (aSEC) chromatography experiments were performed on Superdex 200HR or Sephacryl S-300HR columns (Cytiva). A calibration curve was constructed using the elution volumes of standard proteins and blue dextran (Cytiva; HMV and LMV calibration kit) and their correlation with the void volume of the aSEC column to measure the hydrodynamic radius. SEC-MALS (SEC coupled to a multi-angle light scattering detector), which analysis does not depend on molecular conformation, was used to detect the absolute molecular masses of the proteins. Input samples for aSEC and SEC-MALS were from 3.7 to 6.0 mg mL^{-1}. DLS experiments were made using a Zetasizer Nano ZS ZEN3600 (Malvern) at protein concentrations from 14 to 100 μM. Data were analyzed using both Astra (Wyatt Technology) and Zetasizer Nano (Malvern) software to calculate the diffusion coefficient *D*. DLS measurements were performed at 25°C and were an average of 20 repetitions. Hydrodynamic theoretical parameters were calculated using the Stokes–Einstein equation[44] and considering a non-hydrated sphere.

2.4 | Spectroscopy studies

All experiments were performed in triplicates, using 1–5 mm cuvettes and protein concentrations from 2.3 to 4.1 μM. Circular Dichroism (CD) spectra were recorded in a Jasco-J720 spectropolarimeter, based on standard conditions as previously described.[45] Briefly, each spectrum measurement was accumulated at least 8×, from 260 to 202 nm, at 20°C, velocity of measurement of 20 nm min^{-1}, and response of 1.0 nm. Fluorescence spectra were recorded on a Varian Cary Eclipse Fluorescence Spectrometer with emission wavelengths from 300 to 400 nm, excitation at 295 or 280 nm, and at 25°C. Each measurement was accumulated at least 4×. Thermal-induced unfolding was measured from 20 to 90°C, 1°C min^{-1}, followed by CD signal

at 222 nm. For chemical-induced unfolding, proteins were incubated with urea, 0.0–8.0 M, for 20 min, at 25°C, before measurement.

2.5 | Small-angle X-ray scattering

Small-angle X-ray scattering (SAXS) measurements were performed at the Brazilian Synchrotron Light Laboratory (SAXS beamline at LNLS – CNPEM, Campinas, Brazil; Proposal 20170202) with a monochromatic X-ray beam ($\lambda = 1.488$ Å). The sample-to-detector distance was ~1000 mm, corresponding to the scattering vector range of $0.15 < q < 3.5$ nm^{-1}. All SAXS data were collected with HsHSP110 at 7.5 mg/mL and SbHSP110 at 7.8 mg/mL at room temperature. SAXS curves were corrected by the incident beam intensity, sample's attenuation, and buffer contribution. SAXS data were also checked against radiation damage (by measuring 10 consecutive frames of ~10 s). The final scattering curves were then collected during ~100 s in order to increase the signal-to-noise ratio at large q values. Data analyses were performed with the ATSAS package.[46] The monodispersity was verified by the PRIMUS software.[47] Molecular mass (MM) calculations were performed using the Bayesian inference of different concentration-independent methods, all of which relied on $I(0)$ value.[48] The radius of gyration (Rg) was calculated as previously published.[47,49,50] The pair distance distribution function, $p(r)$, was calculated using GNOM software,[51] which uses the Indirect Fourier Transform methodology.[50]

2.6 | Chaperone activity

Chaperone activity experiments were performed as previously described.[52,53] Client proteins aggregated by temperature (40°C for *Hs*Hsp110 tests and 42°C for *Sb*Hsp110 tests) were citrate synthase (2.0–2.5 μM), malate dehydrogenase (2.5 μM) and luciferase (1.25–2.50 μM). Insulin was aggregated by adding 25 mM dithiothreitol (DTT) at 20°C. The experiments were performed in the absence or presence of HSP110s, at distinct stoichiometry ratios to explore the difference in affinities between chaperone and client proteins and also to avoid scattering caused by high protein concentration. Additionally, BSA and aldolase were used as negative controls (dummy protein replacing the chaperone) for thermal- and DTT-induced aggregation experiments, respectively, and had no significant effects (see text). The aggregation of each client-protein was monitored by light scattering (turbidity) at 320 nm, up to 50 min, using an Aminco-Bowman Series 2 fluorometer equipped with a thermoelectric sample-temperature controller (Peltier system) and a 10 mm × 2 mm quartz cuvette.

2.7 | Refolding assays

Experiments were performed as previously described.[31] Folded (F) luciferase oxides luciferin, which luminescence was monitored using a Biotek Synergy HT luminometer in a 96-well white plate. Luciferase (1.4 μM) was unfolded in buffer (KOAc 100 mM, Hepes-KOH 20 mM, pH 7.5, $Mg(OAc)_2$ 5 mM, and DTT 10 μM) containing 8 M guanidinium-chloride (Gdm-Cl) for 10 min at room temperature and then diluted 100-fold. Unfolded luciferase was then incubated for 1 h at room temperature with 2 mM ATP and (1) HSP70/HSP40 (2 μM each), (2) a mix of HSP70/HSP40/HsHSP110 (2 μM each), (3) a mix of HSP70/HSP40/SbHSP110 (2 μM each), or (4) BSA (bovine serum albumin; dummy protein) as a negative control. Recovery of luciferase enzymatic activity after being unfolded (U) and incubated with chaperones was compared to the activity of the folded (F) enzyme.[24,26] The activity was investigated by taking 8 μL of the sample, mixing it with 100 μL of luciferin at 0.62 mg/mL, and measuring luminescence as a function of time. The activity of folded luciferase was set as 100%.

2.8 | Disaggregation assays

Experiments were performed as previously described.[31] The aggregation of luciferase (2 μM) was induced by heating the protein for 15 min at 45°C in the presence of HSPB1-3D (20 μM), which prevents the formation of non-recoverable luciferase aggregates.[31] The mix was then incubated with 2 mM ATP and (1) HsHSP110 (0.5 μM), HSP70 (2 μM) and HSP40 (1 μM); (2) SbHSP110 (0.5 μM), HSP70 (2 μM) and HSP40 (1 μM); or (3) BSA (bovine serum albumin; dummy protein) at 30°C for up to 3 h. Recovery of luciferase enzymatic activity after aggregation and incubation with chaperones was measured at time points and compared to the activity of the folded (F) enzyme.[24,26] Measurement of activity was done as described in Section 2.7 and the activity of folded luciferase was set as 100%.

3 | RESULTS AND DISCUSSION

3.1 | *Sb*HSP110, HSP110 from *Sorghum bicolor*

The combination of HSP110s and HSP70s constitute a HSP70 superfamily as much of their structure and function characteristics can be deduced from sequence comparison.[22] HSP110s are critical for protein homeostasis in stress and physiological environment and their deletion causes cell lethality.[27,54] Of highly importance, both human and yeast HSP110s are essential to promote protein disaggregation.[23,31]

To increase the general knowledge about the function of HSP110 in plants, a putative gene annotated in *S. bicolor*, one of the most important economical cereal in the world, and its translated sequence, named here *Sb*HSP110, was investigated. Using human HSP110 (UNIPROT Q92598) as query, the putative sequence for *S. bicolor* HSP110 was identified in the NCBI database with the reference XP_002439385.1. *Sb*HSP110 had 842 amino acid residues (about 93 kDa) and shared ~40% of identity with human HSP110 as identified by the MUSCLE software[38] (Figure 2a).

The sorghum HSP110 sequence was compared with those from other species to generate a phylogenetic tree (Figure 2b). *Sb*HSP110

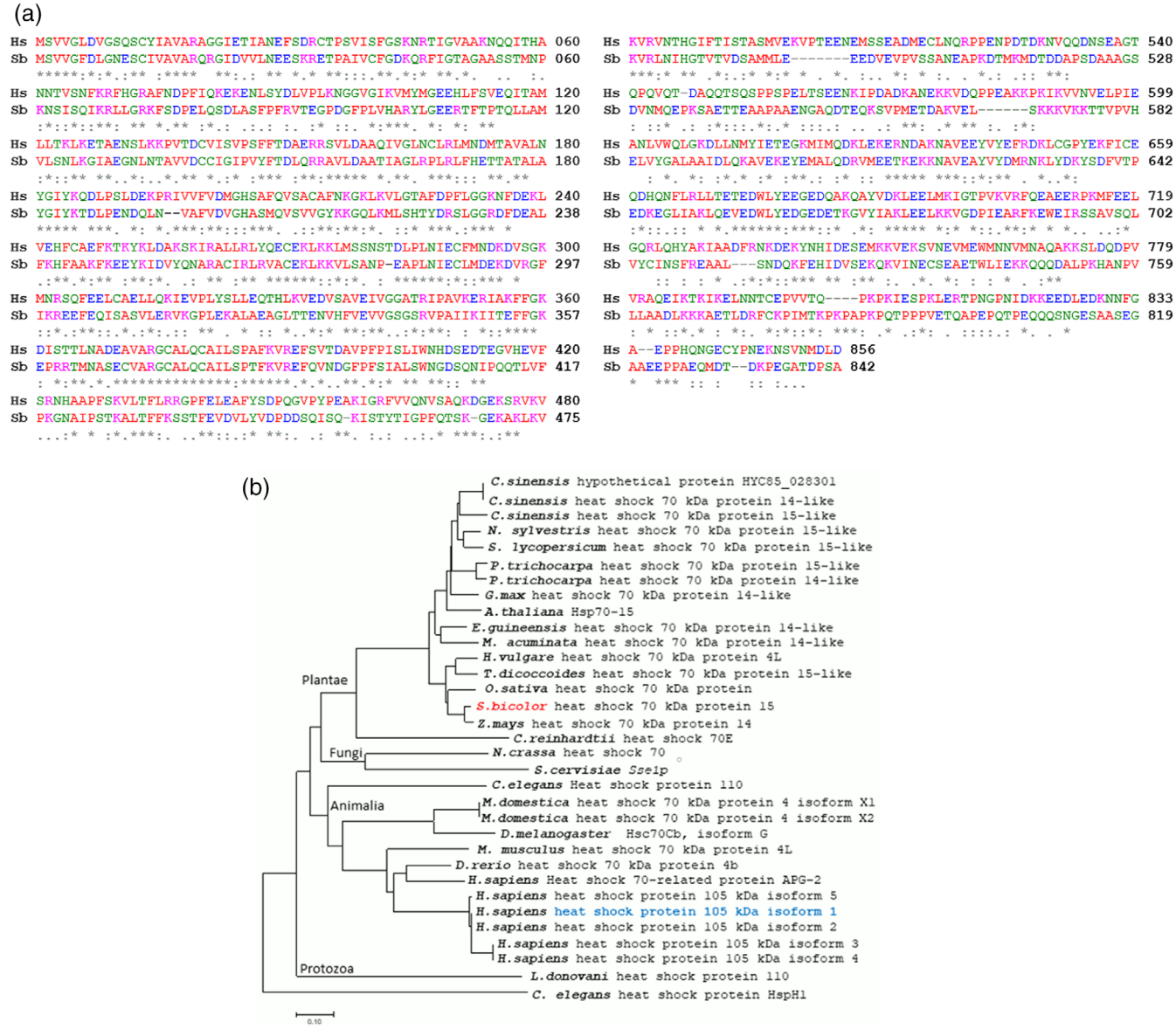

FIGURE 2 (a) Sequence alignment of human (*Hs*) and sorghum (*Sb*) HSP110 proteins. Proteins share approximately 40% identity and 57% similarity, as calculated by the NCBI blastp® webserver (https://blast.ncbi.nlm.nih.gov/Blast.cgi?PAGE=Proteins). Sequences: human HSP110 (UNIPROT Q92598), *Sorghum bicolor* HSP110 (NCBI database XP_002439385.1). The alignment was generated by the MUSCLE webserver.[38] (b) HSP110 phylogenetic tree. Comparison of HSP110 sequences from several organisms. The sorghum and human HSP110s studied in this work are highlighted in red and blue, respectively.

had high similarity with several of their plant homologous: *Zea mays*, *Oryza sativa*, *Triticum dicoccoides*, *Hordeum vulgare*, *Elaeis guineensis*, *G. max*, *Tricoharpa*, *Solanum lycopersicum*, *Nicotiana sylvestris*, *Camellia sinensis*, and *A. thaliana*, suggesting relevant functions in plants. As a matter of fact, HSP110s are constitutively expressed in rice in all stages of development and at least one gene is upregulated under heat stress.[55] The deficiency of HSP70-15 (HSP110) in *A. thaliana* led to a reduced ability to acclimate to high temperature[56] severe growth retardation, and increased mortality upon heat treatment.[57]

To highlight the relevance of our work, we would like to point out that, at the time of writing, the search for HSP110 in the NCBI database (https://www.ncbi.nlm.nih.gov), using nucleotide and plant species parameters, generated only 20 hits and none from sorghum. Searching the PlantGDB/Sorghum Genome database (https://www.plantgdb.org/SbGDB/cgi-bin/search.pl) for HSP110 generated no hits while searching for HSP70 generated 20 hits. Thus, it is likely that other genes for HSP110 in sorghum have not been annotated yet.

3.2 | HSP110s were purified as folded and stable monomers

HSP110s from human and sorghum were cloned into pPROEX-Htb and pET-28a vectors, respectively, expressed in *E. coli* cells and purified

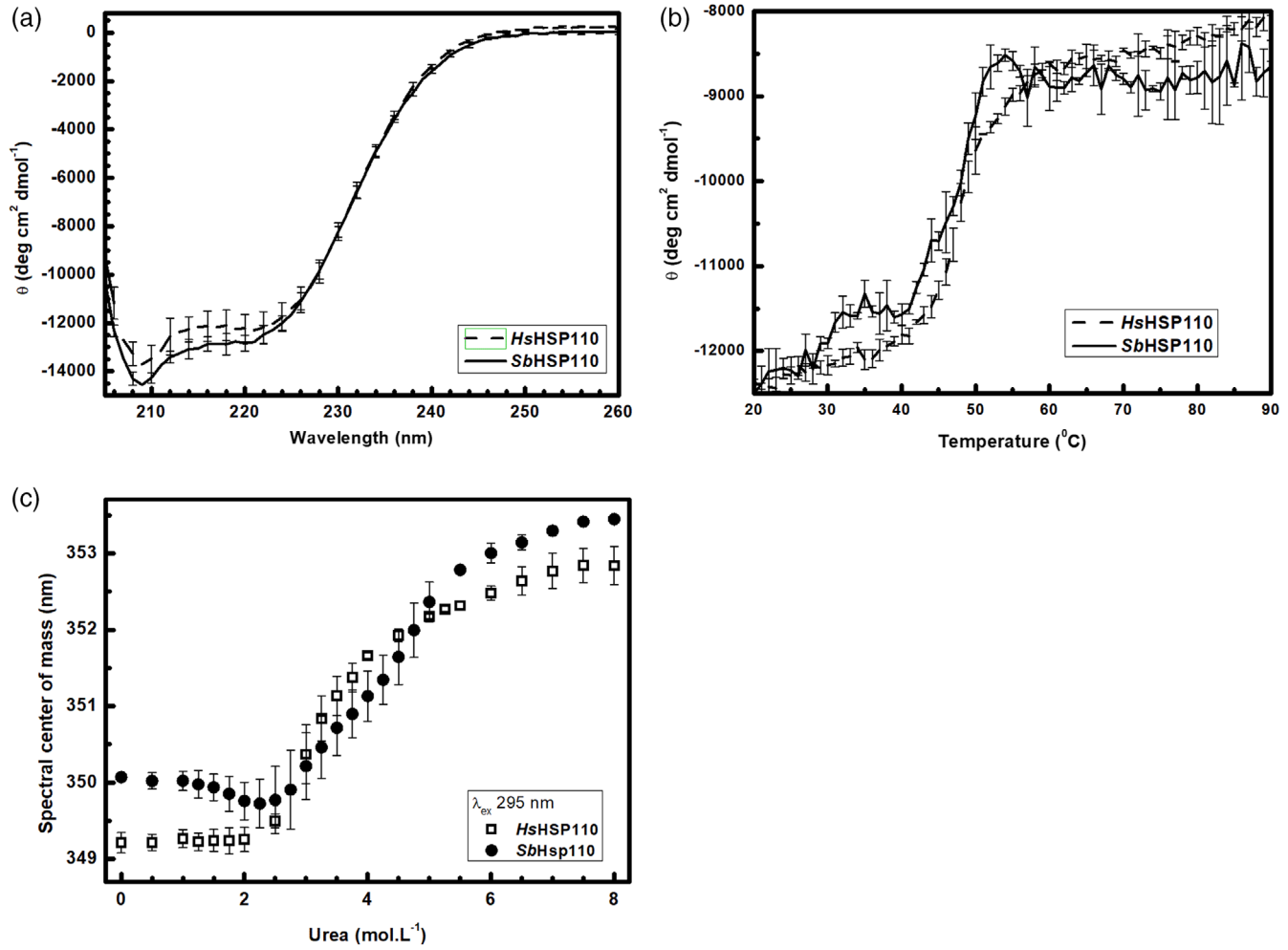

FIGURE 3 HSP110s were folded and stable. (a) Circular dichroism spectra of HsHSP110 and SbHSP110 at 20°C. *Sb*HSP110 and *Hs*HSP110 concentrations were 2.8 and 4.1 μM, respectively. (b) Heat-induced unfolding. Samples were incubated from 20 to 90°C and followed by CD signal at 222 nm. Refolding was irreversible under these conditions (data not shown). (c) Urea-induced unfolding followed by tryptophan fluorescence (center of mass). Urea was added from 0.0 to 8.0 M, and the protein concentrations were 2.5 μM for HsHSP110 and 2.8 μM for *Sb*HSP110. All data are the average of at least three independent experiments with standard deviation errors.

by affinity chromatography. *Hs*HSP110 and *Sb*HSP110 were eluted with 42 and 150 mM Imidazole, respectively, and were more than 95% pure (Figures S1 and S2). The heterologous expressed *Sb*HSP110 had an N-terminal His-tag with 20 amino acid residues and its theoretical molecular mass was approximately 95 kDa.

*Sb*HSP110 secondary structure composition was first analyzed using the Psipred software and the prediction is shown in Figure S3A. Additionally, SMART software predicted a HSP70 domain in *Sb*HSP110 (residues 3–691 with an *E*-value of 3.5e−162. Figure S3B). Circular dichroism (CD) was used to further investigate the secondary structure of both HSP110s, from *H. sapiens* (*Hs*HSP110) and *S. bicolor* (*Sb*HSP110). The spectra of both proteins showed similar CD pattern with two minima at 208 and 222 nm, characteristic of α-helical secondary structure (Figure 3a). The calculated α-helix content using the wavelength of 222 nm was of about 40% for both *Hs*HSP110 and *Sb*HSP110, values near the prediction made in this work (Figure S3A) and also to that of HSP110 Sse1 (UNIPROT Q875V0) from yeast, which is 38%. Combined, these investigations showed that the proteins were purified folded.

Subsequently, the stability of the HSP110 chaperones was investigated. First, the thermal stability was evaluated by performing a heat-induced unfolding experiment, which was monitored by the CD signal at 222 nm from 20 to 90°C (Figure 3b). The thermal-induced profiles of the proteins were similar to each other (Figure 3b) and also to those of *S. cerevisiae* Sse1 and *H. sapiens* Apg-2 Hsp110s,[58] indicating that HSP110s from different organisms may share similar stabilities. The post-transition likely involved aggregation as the signal was still high for an unfolded protein and was not reversible (data not shown). Similar conformational stability was also confirmed by studies using a chemical denaturant. Urea-induced unfolding was followed by tryptophan fluorescence (center of mass; Figure 3c). In all cases, pre-transitions were up to about 2.0 M urea and post-transitions started at about 5.5 M urea (Figure 3c). The transitions were similar inside the error, indicating

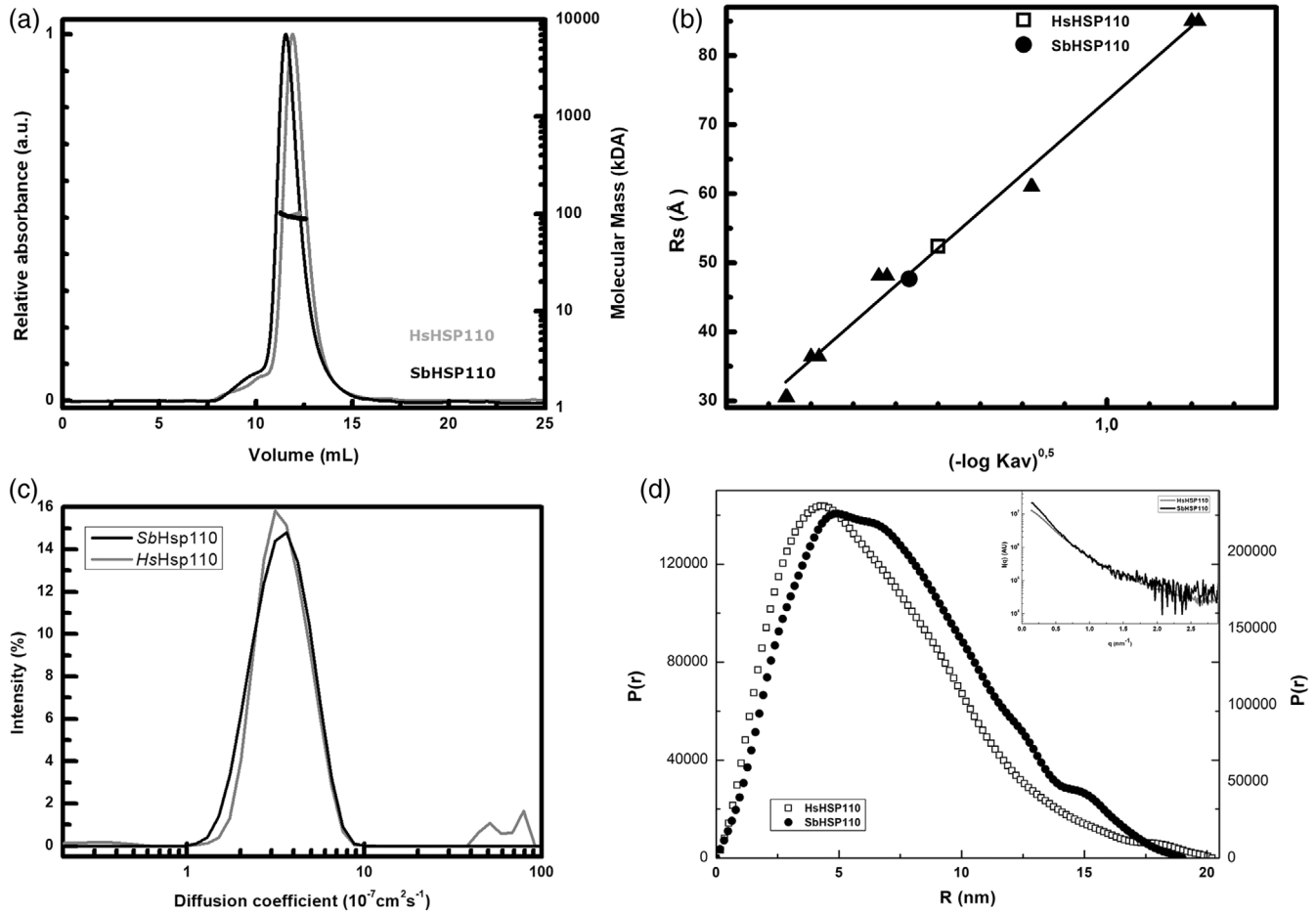

FIGURE 4 HSP110s were elongated monomers in solution. (a) SEC-MALLS analyses, which do not depend on molecular conformation, of monomeric *Hs*HSP110 (gray) and *Sb*HSP110 (black). The SECMALS curves were treated on Astra® (Wyatt) software to generate a graph of the molecular mass distribution as a function of the elution volume of the protein. Both *Hs*HSP110 and *Sb*HSP110 were monomers in solution. (b) Curve of standard and HSP110 proteins based on the data obtained from the Analytical Size Exclusion chromatography indicating their Stokes (or hydrodynamic) radii (R_S). Standard proteins are shown as triangles, and human and sorghum HSP110s are shown as empty squares or filled circles, respectively. (c) The diffusion coefficient (D) values for HsHSP110 (at 64 μM) and *Sb*HSP110 (at 42 μM) obtained by DLS were $3.6 \pm 0.2 \times 10^{-7}$ cm^2 s^{-1} and $3.7 \pm 0.1 \times 10^{-7}$ cm^2 s^{-1}, respectively. (d) $p(r)$ functions obtained by GNOM analysis of SAXS data. Inset: experimental curves.

once again that human and sorghum HSP110s have similar stabilities. Urea-induced unfolding followed by tryptophan fluorescence (center of mass; Figure 3c) also indicated that one or more Trp residues were at least partially buried in the folded conformation (~350 nm) and were exposed to the solvent after unfolding as seen by the increase in wavelength (~353 nm).

The molecular masses (MM) of the folded proteins were evaluated by analytical size exclusion coupled to the multi-angle light scattering (SEC-MALLS) (Figure 4a), an absolute technique for molecular mass determination. The measured MM of *Sb*HSP110 was 98 ± 3 kDa, a value similar to the monomeric value calculated from amino acid composition (95.23 kDa). Similarly, the measured MM of *Hs*HSP110 was 94 ± 2 kDa, a value similar to the monomeric value calculated from amino acid composition (99.96 kDa). These results indicated that HSP110 chaperones, from either sorghum or human, are monomers in solution (Table 1). Many studies in the literature support that HSP110s have monomeric conformation, that is, the monomeric human HSP110 SBD domain crystal.[59]

3.3 | On the conformation of SbHSP110

Since the HSP110s studied here were purified folded, a set of experiments was performed to gain additional information about the overall conformation of these proteins. Both chaperones had Stokes or hydrodynamic radius (R_s) of 4.8 ± 0.1 nm (Figure 4b and Table 1). Diffusion coefficient, D, values, measured by DLS, obtained for *Sb*HSP110 and HsHSP110 were equal to $3.7 \pm 0.1 \times 10^{-7}$ cm^2 s^{-1} and $3.6 \pm 0.2 \times 10^{-7}$ cm^2 s^{-1}, respectively (Figure 4c and Table 1). These values were compared to the values calculated for a hypothetical solid non-hydrated sphere with the same molecular mass (Table 1) because this approach allows verifying whether the conformation of

the protein deviates from a globular shape.[60] The results (Table 1) indicated that the measured parameters were different from those of a sphere and thus that the HSP110s studied here have a nonglobular or elongated shape as observed for other members of the HSP110 family (see for instance Reference [61]).

SAXS experiments (see Figure S4) were used to estimate the molecular masses of the HSP110 proteins: 99.4 kDa for HsHSP110 and 99.5 kDa for SbHSP110 (Table 1), results that were in very good agreement with those from both SEC-MALS and the prediction from the amino acid composition. The Guinier's plot (Figure S4, inset) showed a linear behavior in the small-q range, indicating a monodisperse system for both HSP110s. SAXS analyses also generated the pair-distance distribution function $p(r)$ (Figure 4d), which indicated that both proteins had a non-spherical, quite elongated shape with a D_{max} of 20.2 ± 2.0 and 19.0 ± 2.0 nm for human and sorghum, respectively, HSP110s (Figure 4d and Table 1). From the $p(r)$ is also possible to measure the radius of gyration (Rg), the distribution of atoms of a protein around its axis. HsHSP110 had an Rg of 4.1 ± 0.2 nm, and SbHSP110 had an Rg of 4.7 ± 0.3 nm (Table 1), once again indicating that the proteins have similar conformation. Furthermore, these results can give additional information about the conformation of the proteins as a ratio Rg/R_S higher than 0.775 indicates nonglobular or elongated conformation. The Rg/R_S ratio was 0.85 for HsHSP110 and 0.98 for SbHSP110 (Table 1), one more indication of the nonglobular conformation of these proteins.

TABLE 1 Parameters obtained for HSP110s.

Parameter	HsHSP110	SbHSP110
MM (kDa; from SEC-MALS)	94 ± 2 (99.96)[a]	98 ± 3 (95.23)[a]
MM (kDa; from SAXS)	99.4	99.5
D ($\times 10^{-7}$ cm^2 s^{-1})	3.6 ± 0.2 (5.5)[b]	3.7 ± 0.1 (5.6)[b]
R_s (nm)	4.8 ± 0.1 (3.1)[b]	4.8 ± 0.1 (3.0)[b]
Rg (nm)	4.1 ± 0.2	4.7 ± 0.3
Rg/R_s	0.85 (0.775)[c]	0.98 (0.775)[c]
D_{max} (nm)	20.2 ± 2.0	19.0 ± 2.0

[a]Predicted: from amino acid sequence.
[b]Predicted: for a nonhydrated sphere with the same molecular mass.
[c]Predicted: for a globular protein.

The 3D structure of *Sb*HSP110 was predicted by i-tasser (Figure 5a) and is very similar to the structure prediction for human HSP110 (HSP105) made by AlphaFold (available in the AlphaFold site and also in UNIPROT). The N-terminal domain is a mixture of α-helices and β-sheets while the C-terminal domain is mainly α-helical with a coil extension at the very C-terminus. The overall conformation is in good agreement with the secondary structure prediction by a different predictor (Figure S3), therefore supporting the confidence in the model. The predicted structure for SbHSP110 should be assessed with caution as it may differ from other isoforms, even though it is very similar to that predicted for the human isoform generated by AlphaFold.

Worth noting is the nonglobular conformation of this prediction that is supported by several experimental evidence in this work (see for instance Table 1). Figure 5b shows the positions of the Trp residues in the predicted three-dimensional model of SbHSP110, indicating that the surface of all Trp residues are indeed mostly buried, supporting the Trp fluorescence results described in Figure 3c.

3.4 | *Sb*HSP110 has chaperone activity

One important function of several chaperone families is to protect other proteins from aggregation, a holder activity that is ATP-independent as

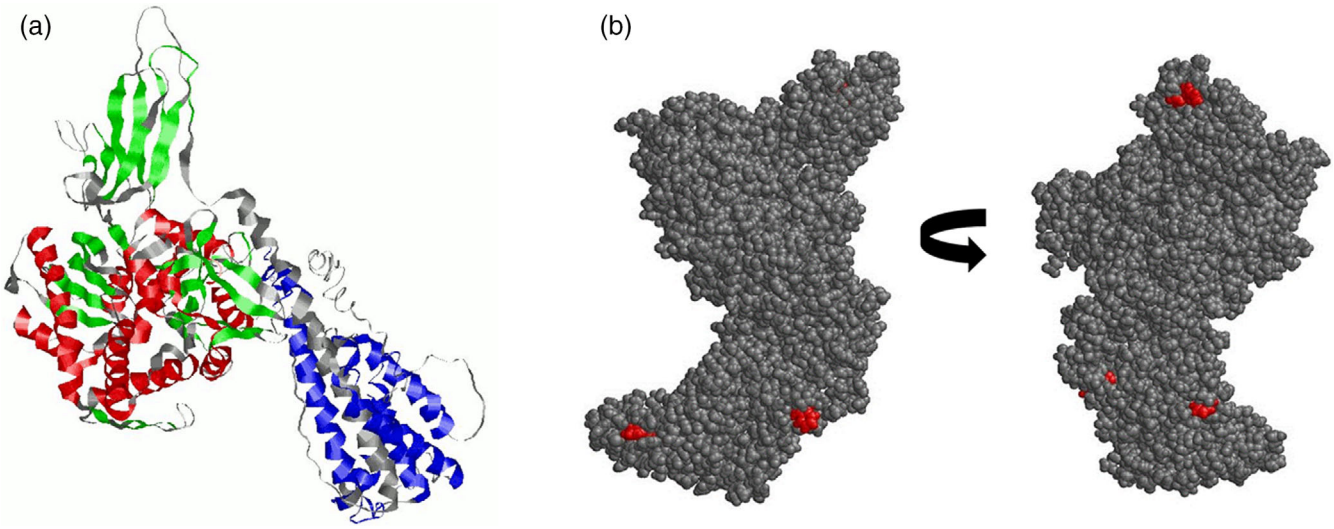

FIGURE 5 (a) In silico prediction structure model of *Sb*HSP110. The N-terminal domain (left) is a mixture of α-helices (red) and β-sheets (green), while the C-terminal domain is mainly alpha-helical (blue and gray) with a coil extension (gray) at the very C-terminus. Structure (by Psipred) and domain (by SMART) predictions are shown in Figure S3. Secondary structure colors (red, green, and blue) are from Psipred prediction. (b) In silico prediction model of *Sb*HSP110. Tryptophan residues (positions 403, 658, 692, and 741 from SbHSP110 numbering) are in red and appear to be at least partially buried.

previously verified by other HSP110 investigations (see for instance Reference [54]) and other holder chaperones such as HSP40s/DNAJs and SmallHSPs. We evaluated the efficiency of SbHSP110 in protecting well-characterized client proteins against thermal- and redox-induced aggregation and compared the results with those of HsHSP110 (Figure 6a). The studied HSP110s had similarities in preventing the aggregation of some of the client proteins studied here. Both Hsp110s were very efficient in preventing the thermal-induced aggregation of CS, more than 95% protection was reached (Figure 6a), and in preventing the redox-induced aggregation of insulin (Figure 6a). However, the studied HSP110s had differences in preventing the aggregation of the other client proteins studied here. At the same ratio, HsHsp110 was more efficient in preventing the thermal-induced aggregation of luciferase than SbHsp110 while SbHsp110 was more efficient in preventing the thermal-induced aggregation of MDH than HsHSP110 (Figure 6a). The experiments were also done in the absence or presence of ATP (1× and 10×) but no significant difference was noted, as expected for a holder activity. Nonetheless, in the conditions tested here, SbHSP110

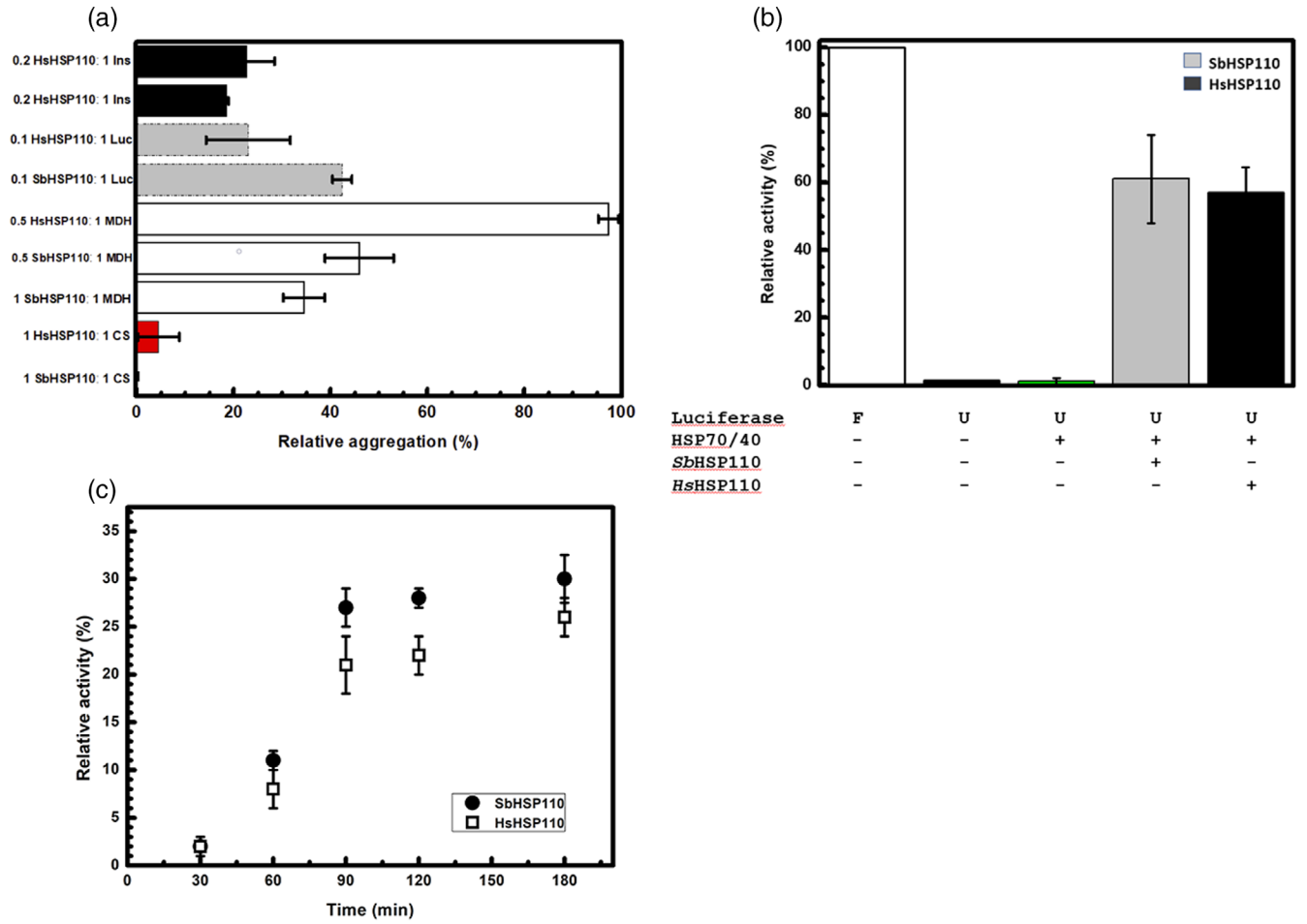

FIGURE 6 (a) Chaperone activity of HSP110s. The chaperone activity from human and sorghum HSP110 was tested with the model proteins citrate synthase (CS, red columns), malate dehydrogenase (MD, white columns), luciferase (Luc, gray columns), and insulin (Ins, black columns) (see Figure S5 for examples of raw data). The proteins were heated in the absence and in the presence of chaperones, and light scattering (turbidity) was collected for 50 min. The chaperone activity in preventing redox-induced aggregation was tested using insulin, which was incubated with DTT in the absence and in the presence of chaperones, and light scattering (turbidity) was collected for 50 min. The aggregation in the absence of chaperones was set at 100%, and the results are shown as relative aggregation as a function of HSP110:client protein ratio indicated at the side of the figure. Experiments were also done in the presence of BSA (heat-induced) or aldolase (DTT-induced) as negative controls of chaperones, with no significant effect (Figure S5). (b) Refolding of luciferase chemical-induced aggregates. Folded (F) luciferase was unfolded (U) with Gdm-Cl. Samples were incubated for 1 h at room temperature in the presence and in the absence of combined chaperones (HSP110 and HSP70/HSP40). The activity of samples to convert the substrate luciferin was measured by luminescence emission and plotted as a function of folded luciferase (F), which was 100%. Refolding was partial and only reached when HSP110 (*Sb*HSP110, light gray or *Hs*HSP110, black) were added. BSA was used as a negative control of the combined chaperones and was not able to refold luciferase (U column). See Table S1 for more information. (c) Reactivation of luciferase. Aggregated luciferase in the presence of HSPB1-3D, was reactivated when incubated with HSP70/HSP40/HSP110, either using *Sb*HSP110 (gray) or *Hs*HSP110 (black). Measurements of the recovery of the luciferase enzymatic activity were taken every 30 min until the final record at 180 min. The data presented refer to the average of at least three independent experiments with a standard error of the mean. See Table S2 for more information.

was effective in preventing both heat- and redox-induced aggregation of a broad variety of substrates and, in general, was as efficient as HsHSP110.

3.5 | *Sb*HSP110 replaces human HSP110 in disaggregation and refolding assays

To further investigate the chaperone activity of SbHSP110, the ability of the chaperone in participating in disaggregating and refolding chaperone machines was studied. The SbHSP110 results were compared to those of HsHSP110. For that, the chaperone machinery consisted of HSP110 (Sb or Hs), HSP70, and HSP40, both from human, and the client protein tested was luciferase that, when folded (F), oxides luciferin, which emits luminescence. Unfolded (U) or aggregated luciferase lost its enzymatic activity, which can be recovered when the protein is reactivated by the chaperone machinery. The experiments were performed in the presence of ATP since the HSP70-base machinery is dependent on ATP as expected for foldases and disagregases.[23,26] The disaggregation and reactivation activities were observed in the absence of ATP or substitution for non-hydrolyzable analog, such as AMP-PNP as previously reported.[22,31]

First, the chaperone effects were tested on luciferase chemically unfolded (U) by Gdm-Cl (Figure 6b). The activity of folded luciferase (F; Figure 6b, first column) was set as 100%. Unfolded luciferase (U; Figure 5b, second column) in the absence of chaperones, or presence of BSA (control) had of about 1% activity. The presence of HSP70/HSP40 (third column in Figure 6b) had no significant effect on the refolding of luciferase. However, the addition of HSP110, either SbHSP110 (fourth column in Figure 6b) or HsHSP110 (fifth column in Figure 6b), to HSP70/HSP40, formed an efficient chaperone machinery that was capable to refold luciferase recovering of about 55% and 45%, respectively, of its activity (Figure 6b).

Next, the ability of SbHSP110 to participate in a chaperone machinery capable to reactivate aggregated luciferase was tested. For that, luciferase was aggregated at 45°C in presence of the small HSP HSPB1-3D, which is required to improve the recovery of luciferase aggregates.[31] As a matter of fact, stress-induced phosphorylation of three serine sites (Ser15, Ser78, and Ser82) is essential for the activation of the HSPB1 chaperone function by inducing dissociation of oligomers into dimers and enabling substrate binding.[62]

Each aggregated luciferase sample was incubated up to 180 min as follows: alone; with BSA, used as a negative control; with each HSP110 alone; with only HSP70/HSP40; and with the HSP70/HSP40/HSP110 machinery. Luminesce emission was measured to evaluate the amount of luciferase that was reactivated in the process and plotted as a function of time points (Figure 6c). BSA, HSP110 or HSP70/HSP40 had no significant effect in reactivating luciferase (see Supplementary material). However, aggregated luciferase incubated with HSP70/HSP40/HSP110, either using SbHSP110 (gray) or HsHSP110 (black), showed reactivation and these results, as a function of time points, are shown in Figure 6c. Altogether, the results support the hypothesis that plants have more than one chaperone system capable of acting on the reactivation of protein aggregates.

The finding that HSP110s participate in disaggregation machineries is new and not yet completely understood, thus we decide to first explore this investigation on SbHSP110. The NEF activity of a sorghum HSP110 is also important, demands a new and laborious experimental set up and therefore will be the goal of future investigations.

4 | CONCLUSIONS

A putative gene from *S. bicolor* coding for HSP110 was found by searching the plant genome with the human HSP110 sequence. The cDNA was cloned in an *E. coli* expression vector and the recombinant protein was expressed. The protein, *Sb*HSP110 was purified folded, and characterized in comparison with human *Hs*HSP110. *Sb*HSP110 was similar to *Hs*HSP110 regarding conformation and stability, both were monomeric with nonglobular, or elongated, shapes, an observation confirmed by several biophysical tools used in the investigation. The high amino acid sequence identity between the proteins and the high conformational similarity are already strong indicators that validate the putative gene as a HSP110. The functional characterization of SbHSP110 gave a solid validation to this hypothesis.

*Sb*HSP110 showed chaperone activity, as it was able to protect client-proteins from aggregation. Furthermore, *Sb*HSP110 was able to participate with a set of other chaperones, HSP70/HSP40 and HSP70/HSP40/HSPB1-3D, to provide refolding and reactivation of both unfolded and aggregated luciferase, a model protein to investigate the functional activity of HSPs. In these experiments *Sb*HSP110 had functional activity at least equal to that of HsHSP110, being able to surpass the human chaperone in some specific experiments. Although there are still few studies on plant HSP110s, the results herein are in good agreement with the experimental evidence of the importance of this family of chaperones in plants.

Altogether, the results not only confirmed that *S. bicolor* had a functional HSP110 gene but that the protein may be an additional player in the reactivation of aggregates, a distinctive function of HSP100 which, although present in plants, appear to be missing in protozoans.

AUTHOR CONTRIBUTIONS

Data collection, analysis, and interpretation: Juliana C. Franco, Maria L. C. Nogueira, Gabriela M. Gandelini, Glaucia M. S. Pinheiro, Conrado C. Gonçalves; Data analysis and interpretation: Leandro R. S. Barbosa, Jason C. Young; Data analysis and interpretation and design of the work: Carlos H. I. Ramos; All authors: drafted and critically reviewed the article.

ACKNOWLEDGMENTS

This work was supported by FAPESP (2012/50161-8; 2017/26131-5). Carlos H. I. Ramos and Leandro R. S. Barbosa have research fellowships from CNPq (305148-2019-2 and 309418/2021-6, respectively). The following authors received research fellowship from

FAPESP: Juliana C. Franco (2016/02137-1), Maria L. C. Nogueira (2016/14503-2), Gabriela M. Gandelini (2016/04246-2), Glaucia M. S. Pinheiro (2018/11948-9), and Conrado C. Gonçalves (2016/03764-0) received fellowship from FAPESP. The authors thank Annelize Z B Aragão for critical suggestions and technical assistance. This research used facilities of the Brazilian Synchrotron Light Laboratory (LNLS), part of the Brazilian Center for Research in Energy and Materials (CNPEM), a private non-profit organization under the supervision of the Brazilian Ministry of Science, Technology and Innovations (MCTI). The SAXS1 beamline staff is acknowledged for their assistance during the experiments (proposal 20170202).

CONFLICT OF INTEREST STATEMENT

The authors declare no competing interests.

DATA AVAILABILITY STATEMENT

The data that support the findings of this study are openly available in REDU at https://redu.unicamp.br/dataset.xhtml?persistentId=doi:10.25824/redu/SSXSNM. The data that supports the findings of this study are available in the Supplementary material of this article. Other data that support the findings of this study are available from the corresponding author upon reasonable request.

ORCID

Carlos H. I. Ramos https://orcid.org/0000-0002-7246-9081

REFERENCES

[1] C. H. I. Ramos, S. T. Ferreira, *Protein Pept. Lett.* **2005**, *12*, 213.
[2] L. M. Luheshi, D. C. Crowther, C. M. Dobson, *Curr. Opin. Chem. Biol.* **2008**, *12*, 25.
[3] A. Marino Gammazza, C. C. Bavisotto, R. Barone, E. C. de Macario, A. J. L. Macario, *Curr. Pharm. Des.* **2016**, *22*, 4040.
[4] J. M. Barral, S. A. Broadley, G. Schaffar, F. U. Hartl, *Semin. Cell Dev. Biol.* **2004**, *15*, 17.
[5] P. Csermely, C. Söti, G. L. Blatch, *Adv. Exp. Med. Biol.* **2007**, *594*, 55.
[6] C. Leidhold, W. Voos, *Ann. N. Y. Acad. Sci.* **2007**, *1113*, 72.
[7] A. O. Tiroli-Cepeda, C. H. I. Ramos, *Protein Pept. Lett.* **2011**, *18*, 101.
[8] D. Z. Mokry, J. Abrahao, C. H. I. Ramos, *An. Acad. Bras. Cienc.* **2015**, *87*, 1273.
[9] K. P. da Silva, J. C. Borges, *Protein Pept. Lett.* **2011**, *18*, 132.
[10] L. Shrestha, J. C. Young, *Curr. Top. Med. Chem.* **2016**, *16*, 2812.
[11] E. R. P. Zuiderweg, L. E. Hightower, J. E. Gestwicki, *Cell Stress Chaperon.* **2017**, *22*, 173.
[12] R. Rosenzweig, N. B. Nillegoda, M. P. Mayer, B. Bukau, *Nat. Rev. Mol. Cell Biol.* **2019**, *20*, 665.
[13] D. M. Cyr, C. H. Ramos, *Subcell Biochem.* **2015**, *78*, 91.
[14] H. H. Kampinga, C. Andreasson, A. Barducci, M. E. Cheetham, D. Cyr, C. Emanuelsson, P. Genevaux, J. E. Gestwicki, P. Goloubinoff, J. Huerta-Cepas, J. Kirstein, K. Liberek, M. P. Mayer, K. Nagata, N. B. Nillegoda, P. Pulido, C. Ramos, P. De Los Rios, S. Rospert, R. Rosenzweig, C. Sahi, M. Taipale, B. Tomiczek, R. Ushioda, J. C. Young, R. Zimmermann, A. Zylicz, M. Zylicz, E. A. Craig, J. Marszalek, *Cell Stress Chaperon.* **2019**, *24*, 7.
[15] S. Polier, Z. Dragovic, F. U. Hartl, A. Bracher, *Cell* **2008**, *133*, 1068.
[16] M. P. Mayer, *Trends Biochem. Sci.* **2013**, *38*, 507.
[17] J. N. Rauch, J. E. Gestwicki, *J. Biol. Chem.* **2014**, *289*, 1402.
[18] D. Lee-Yoon, D. Easton, M. Murawski, R. Burd, J. R. Subjeck, *J. Biol. Chem.* **1995**, *270*, 15725.
[19] A. Bracher, J. Verghese, *Front. Mol. Biosci.* **2015**, *2*, 10.
[20] L. Shaner, R. Sousa, K. A. Morano, *Biochemistry* **2006**, *45*, 15075.
[21] S. Storozhenko, P. De Pauw, S. Kushnir, M. Van Montagu, D. Inzé, *FEBS Lett.* **1996**, *390*, 113.
[22] D. P. Easton, Y. Kaneko, J. R. Subjeck, *Cell Stress Chaperon.* **2000**, *5*, 276.
[23] J. Shorter, *PLoS One* **2011**, *6*, e26319.
[24] H. Rampelt, J. Kirstein-Miles, N. B. Nillegoda, K. Chi, S. R. Scholz, R. I. Morimoto, B. Bukau, *EMBO J.* **2012**, *31*, 4221.
[25] M. P. Torrente, J. Shorter, *Prion* **2013**, *7*, 457.
[26] N. B. Nillegoda, J. Kirstein, A. Szlachcic, M. Berynskyy, A. Stank, F. Stengel, K. Arnsburg, X. Gao, A. Scior, R. Aebersold, D. L. Guilbride, R. C. Wade, R. I. Morimoto, M. P. Mayer, B. Bukau, *Nature* **2015**, *524*, 247.
[27] A. Mogk, B. Bukau, H. H. Kampinga, *Mol. Cell* **2018**, *69*, 214.
[28] V. M. Garcia, N. B. Nillegoda, B. Bukau, K. A. Morano, *Mol. Biol. Cell* **2017**, *28*, 2066.
[29] X. Gao, M. Carroni, C. Nussbaum-Krammer, A. Mogk, N. B. Nillegoda, A. Szlachcic, D. L. Guilbride, H. R. Saibil, M. P. Mayer, B. Bukau, *Mol. Cell* **2015**, *59*, 781.
[30] M. L. C. Nogueira, J. C. Franco, G. de Mello Gandelini, C. H. I. Ramos, in *Regul. Heat Shock Protein Responses* (Eds: A. A. A. Asea, P. Kaur), Springer International Publishing, Cham, Switzerland **2018**, p. 155.
[31] C. C. Goncalves, I. Sharon, T. M. Schmeing, C. H. I. Ramos, J. C. Young, *Sci. Rep.* **2021**, *11*, 17139.
[32] D. A. Parsell, A. S. Kowal, M. A. Singer, S. Lindquist, *Nature* **1994**, *372*, 475.
[33] W. B. Gurley, *Plant Cell* **2000**, *12*, 457.
[34] D. Z. Mokry, V. C. H. da Silva, J. Abrahão, C. H. I. Ramos, *J. Plant Biochem. Biotechnol.* **2017**, *26*, 478.
[35] J. C. Borges, C. H. I. Ramos, *Protein Pept. Lett.* **2005**, *12*, 257.
[36] J. C. Borges, C. H. I. Ramos, *Arch. Biochem. Biophys.* **2006**, *452*, 46.
[37] H. Edelhoch, *Biochemistry* **1967**, *6*, 1948.
[38] F. Madeira, Y. M. Park, J. Lee, N. Buso, T. Gur, N. Madhusoodanan, P. Basutkar, A. R. N. Tivey, S. C. Potter, R. D. Finn, R. Lopez, *Nucleic Acids Res.* **2019**, *47*, W636.
[39] D. Xavier Robert, *Nucleic Acids Res.* **2014**, *42*, W320.
[40] I. Letunic, P. Bork, *Nucleic Acids Res.* **2017**, *46*, D493.
[41] Y. Z. NoA Roy, A. Kucukural, *Nat. Protoc.* **2010**, *5*, 725.
[42] D. T. Jones, *J. Mol. Biol.* **1999**, *292*, 195.
[43] T. M. Laue, B. Shah, T. M. Ridgeway, S. L. Pelletier, in *Anal. Ultracentrifugation Biochem. Polym. Sci* (Eds: J. Harding, S. Rowe, A. Horton), Royal Society of Chemistry, Cambridge, UK **1992**, p. 90.
[44] J. T. Edward, *J. Chem. Educ.* **1970**, *47*, 261.
[45] D. H. A. Corrêa, C. H. I. Ramos, *Afr. J. Biochem. Res.* **2009**, *3*, 164.
[46] D. Franke, M. V. Petoukhov, P. V. Konarev, A. Panjkovich, A. Tuukkanen, H. D. T. Mertens, A. G. Kikhney, N. R. Hajizadeh, J. M. Franklin, C. M. Jeffries, D. I. Svergun, *J. Appl. Crystallogr.* **2017**, *50*, 1212.
[47] P. V. Konarev, V. V. Volkov, A. V. Sokolova, M. H. J. Koch, D. I. Svergun, *J. Appl. Crystallogr.* **2003**, *36*, 1277.
[48] H. Fischer, M. Neto, H. B. Napolitano, I. Polikarpov, A. Craievich, *J. Appl. Crystallogr.* **2010**, *43*, 101.
[49] A. Guinier, G. Fournet, *J. Polym. Sci.* **1955**, *19*, 594.
[50] O. Glatter Kratky, *Small Angle X-ray Scattering*, Academic Press, London; New York **1982**.
[51] D. I. Svergun, *J. Appl. Crystallogr.* **1992**, *25*, 495.
[52] A. O. Tiroli, C. H. I. Ramos, *Int. J. Biochem. Cell Biol.* **2007**, *39*, 818.
[53] G. M. S. Pinheiro, C. H. I. Ramos, *Plant Physiol. Biochem. PPB* **2018**, *129*, 285.
[54] H. Raviol, H. Sadlish, F. Rodriguez, M. P. Mayer, B. Bukau, *EMBO J.* **2006**, *25*, 2510.
[55] N. K. Sarkar, P. Kundnani, A. Grover, *Cell Stress Chaperon.* **2013**, *18*, 427.
[56] J. Larkindale, E. Vierling, *Plant Physiol.* **2008**, *146*, 748.

[57] I. Jungkunz, K. Link, F. Vogel, L. M. Voll, S. Sonnewald, U. Sonnewald, *Plant J.* **2011**, *66*, 983.
[58] H. Raviol, B. Bukau, M. P. Mayer, *FEBS Lett.* **2006**, *580*, 168.
[59] G. J. Gozzi, D. Gonzalez, C. Boudesco, A. M. M. Dias, G. Gotthard, B. Uyanik, L. Dondaine, G. Marcion, F. Hermetet, C. Denis, L. Hardy, P. Suzanne, R. Douhard, G. Jego, L. Dubrez, O. N. Demidov, F. Neiers, L. Briand, J. Sopková-de Oliveira Santos, A.-S. Voisin-Chiret, C. Garrido, *Cell Death Differ.* **2020**, *27*, 117.
[60] J. C. Borges, C. H. I. Ramos, *Curr. Med. Chem.* **2011**, *18*, 1276.
[61] Q. Liu, W. A. Hendrickson, *Cell* **2007**, *131*, 106.
[62] R. Freilich, M. Betegon, E. Tse, S.-A. Mok, O. Julien, D. A. Agard, D. R. Southworth, K. Takeuchi, J. E. Gestwicki, *Nat. Commun.* **2018**, *9*, 4563.

SUPPORTING INFORMATION

Additional supporting information can be found online in the Supporting Information section at the end of this article.

How to cite this article: J. C. Franco, M. L. C. Nogueira, G. M. Gandelini, G. M. S. Pinheiro, C. C. Gonçalves, L. R. S. Barbosa, J. C. Young, C. H. I. Ramos, *Biopolymers* **2023**, *114*(2), e23532. https://doi.org/10.1002/bip.23532